Supporting Informations

Electronic Absorption and EPR Spectra.

The complex $[Cu(5,6\text{-dmp})_3]^{2+}$ **2** in 10% DMF/5 mM Tris-HCl/50 mM NaCl aqueous buffer solution shows a broad ligand field band around 680 nm (Table S1), which is in agreement with the square based geometry observed in its X-ray crystal structure. The phen (**1)** and dpq (**3)** analogues also show a single LF spectral feature around 712 and 728 nm (Table S1). The higher LF energy of **2** is expected of its stronger Cu-N bond (cf. above). The ligand-based bands are observed around 267 (**1**), 280 (**2**) and 296 nm (**3**). The analogues Zn(II) complexes also exhibit ligand-based bands around values closer to their Cu(II) analogues. The EPR spectra of **1 – 3** in frozen CH_3CN:acetone solutions are axial [$g_{\|} > g_{\perp} > 2.023$, $G = (g_{\|}\text{-}2)/(g_{\perp}\text{-}2) \approx 3.8$] [1], which is in agreement with the absorption spectral data and the X-ray crystal structures of **1** and **2**. The $g_{\|}$ and $A_{\|}$ values expected for a CuN_4 chromophore [1] are respectively 2.200 and 200×10^{-4} cm^{-1} and the $g_{\|}$ value is expected to increase and the $A_{\|}$ value to decrease on strong axial interaction by nitrogen. Thus the EPR spectral parameters of the present complexes ($g_{\|}$ 2.264 – 2.278; $A_{\|}$ 161 – 174×10^{-4} cm^{-1}) are consistent with the tetragonal distortion observed in the X-ray structure and the value of the structural index $g_{\|}/A_{\|}$ quotient (**1**, 140; **2**, 130; **3**, 141 cm) is consistent with the planarity of CuN_4 basal plane of the complexes.

Reference

1. M. Palaniandavar, T. Pandian, M. Lakhsminarayanan and H. Manohar, *J. C. S. Dalton Trans*., 1995, 455.

Table S1. Electronic absorption and EPR spectral properties [a] of Cu(II) and Zn(II) complexes

Complex		λ_{max} in nm (ε, M^{-1} cm^{-1})		EPR spectra [d]	
		Ligand field [b]	Ligand based [c]		
$[Cu(phen)_3]^{2+}$	**1**	712 (108)	267 (90150)	$g_{\|}$	2.278
			294 sh	$A_{\|}$	164
				$g_{\perp}$	2.073
$[Cu(5,6\text{-}dmp)_3]^{2+}$	**2**	680 (58)	280 (679840)	$g_{\|}$	2.264
			351 sh	$A_{\|}$	174
				$g_{\perp}$	2.084
$[Cu(dpq)_3]^{2+}$	**3**	728 (99)	254 (60858)	$g_{\|}$	2.270
			296 sh	$A_{\|}$	161
				$g_{\perp}$	2.084
$[Zn(phen)_3]^{2+}$	**4**	—	267 (30500)		—
			230 (32300)		
$[Zn(5,6\text{-}dmp)_3]^{2+}$	**5**	—	278 (91260)		—
			298 (95460)		
$[Zn(dpq)_3]^{2+}$	**6**	—	255(55465)		—

[a] In DMF - buffer solution. [b]Concentration, 5×10^{-3} mol.dm^3. [c] Concentration, 2×10^{-5} mol.dm^3. [d] Acetonitrile/acetone (4:1 V/V) glass at 77 K, $A_{\|}$ in 10^{-4} cm^{-1}.

Table S2. Electrochemical behaviour of [a] the copper(II) complexes on interaction with CT DNA at R = [DNA]/[Cu] = 3

Complexes		R	E_{pa} (V)	E_{pc} (V)	$E_{1/2}$ (V)		ΔE_p (mV)	K_{2+}/K_{+}
					CV	DPV[b]		
$[Cu(phen)_3]^{2+}$	**1**	0	0.040	-0.084	0.022	0.021	124	1.17
		3	0.038	-0.066	0.014	0.017	104	
$[Cu(5,6\text{-}dmp)_3]^{2+}$	**2**	0	-0.004	-0.098	-0.051	-0.031	94	3.49
		3	-0.014	-0.102	-0.063	-0.063	88	
$[Cu(dpq)_3]^{2+}$	**3**	0	0.118	0.006	0.062	0.065	112	1.78
		3	0.110	0.036	0.073	0.072	146	

[a] Measured vs. sat. calomel electrode, using glassy carbon electrode scan rate, 50 mV^{-1}; supporting electrolyte 10% DMF : 5 mM Tris-HCl/50 mM NaCl; Complex concentration: 5 x 10^{-4} $mol.dm^3$;
[b] Differential pulse voltammetry (DPV), scan rate 1 mV s^{-1}, pulse height 50 mV.

Table S3. Concentration dependent oxidative cleavage data of SC pUC19 DNA (40 μM, in base pair) by complexes **2** in the presence of ascorbic acid.

		Form (%)	
Serial no	Reaction conditions	SC	NC
1	DNA control	91.8	8.2
2	DNA + H_2A	90.8	9.2
3	DNA + **2** (10 μM)	86.8	13.2
4	DNA + **2** (20 μM)	83.4	16.6
5	DNA + **2** (30 μM)	52.8	47.2
6	DNA + **2** (40 μM)	45.8	54.2
7	DNA + **2** (50 μM)	43.0	57.0

Table S4. Concentration dependent oxidative cleavage data of SC pUC19 DNA (40 μM, in base pair) by complexes **3** (30 μM) in the presence of ascorbic acid.

		Form(%)	
Serial no	Reaction conditions	SC	NC
1	DNA control	91. 8	8. 2
2	DNA + H_2A	90. 8	9. 2
3	DNA + **3 (**10 μM)	2. 3	97. 7
4	DNA + **3** (20 μM)	1. 3	98. 7
5	DNA + **3** (30 μM)	0. 3	99. 7
6	DNA +**3** (40 μM)	-	-
7	DNA +**3** (50 μM)	-	-

Figure S1. The effect of CT DNA on the absorption spectra of complexes of **1 - 6 (**R = [DNA]/[complex] = 25) .

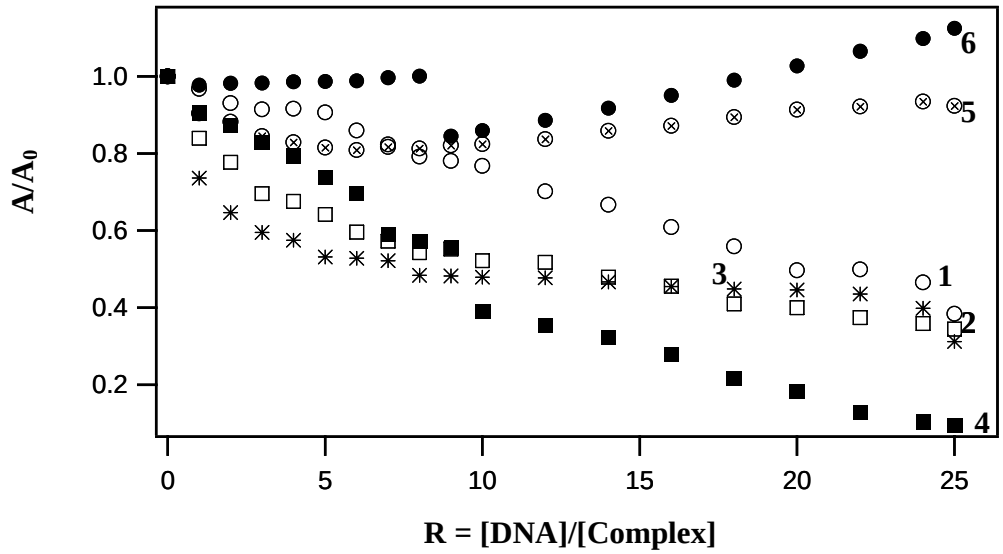

Figure S2. Effect of addition of complex **2** and **5** on the CD intensity of the CT DNA at different complex concentrations in a 5mM Tris-HCl/ 50 mM NaCl buffer at pH = 7.1 at 25 °C

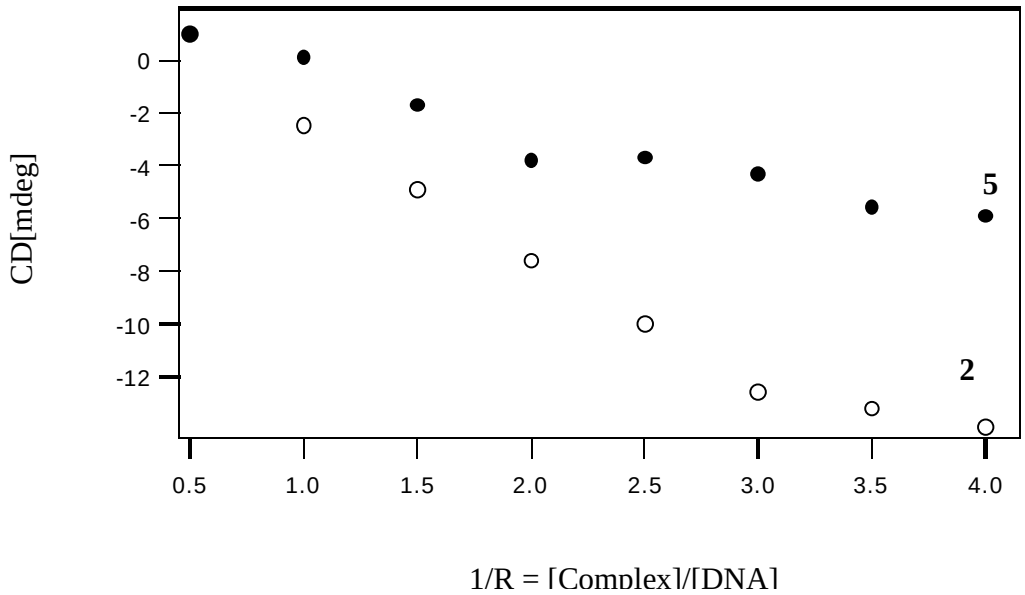

Figure S3A Circular Dichroism spectra of CT DNA in the absence (a) and presence of (b) $[Cu(phen)_3]^{2+}$ (1/R = 2); Conc. of CT DNA = 2 x 10^{-5} mol.dm^3

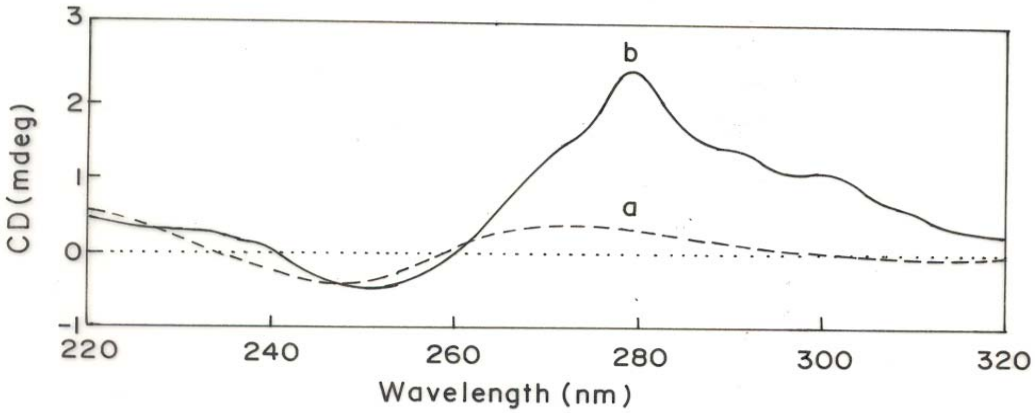

Figure S3B Circular Dichroism spectra of CT DNA in the absence (a) and presence of (b) $[Zn(phen)_3]^{2+}$ (1/R = 2); Conc. of CT DNA = 2 x 10^{-5} mol.dm^3

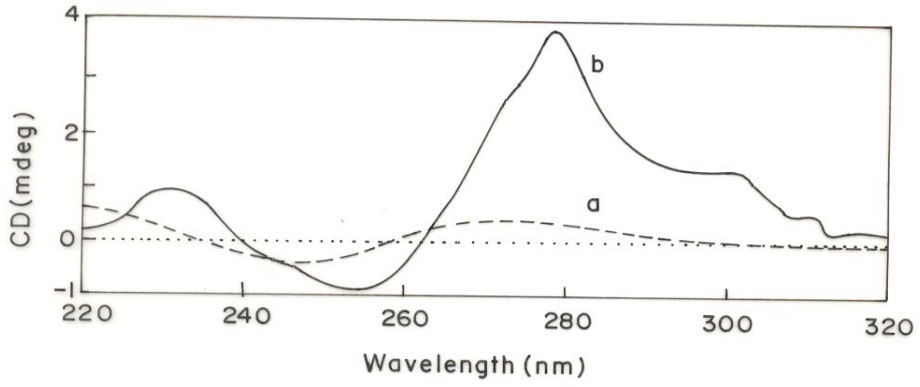

Figure S4. Circular Dichroism spectra of CT DNA, $d(AT)_{12}$, $d(GC)_{12}$ and $d(GTCGAC)_2$ in the absence (a) and presence of the *rac*-$[Zn(5,6\text{-dmp})_3]^{2+}$ (b) Conc of the olynucleotides = 2 x 10^{-5} mol.dm^3 ; Cell length = 0.2 cm

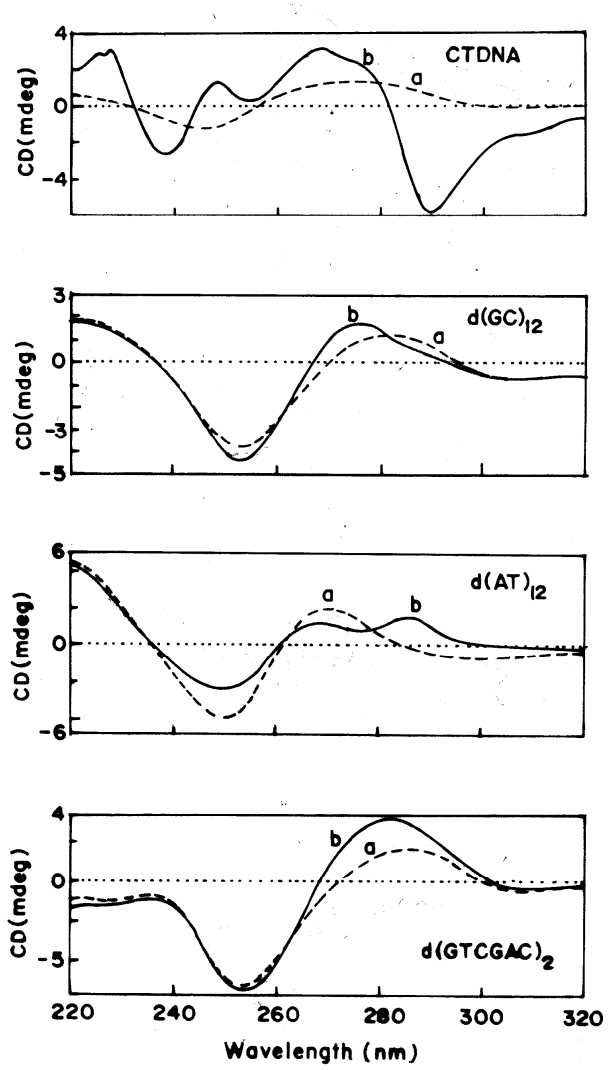

Figure S5A. Circular Dichroism spectra of CT DNA in the absence (a) and presence of *rac*-$[Cu(5,6\text{-dmp})_3]^{2+}$ at 1/R = 2 (b) and of CT DNA incubated with EthBr in the presence of *rac*-$[Cu(5,6\text{-dmp})_3]^{2+}$ at 1/R = 2 (c). Conc. of CT DNA = 2 x 10^{-5} mol.dm^3.

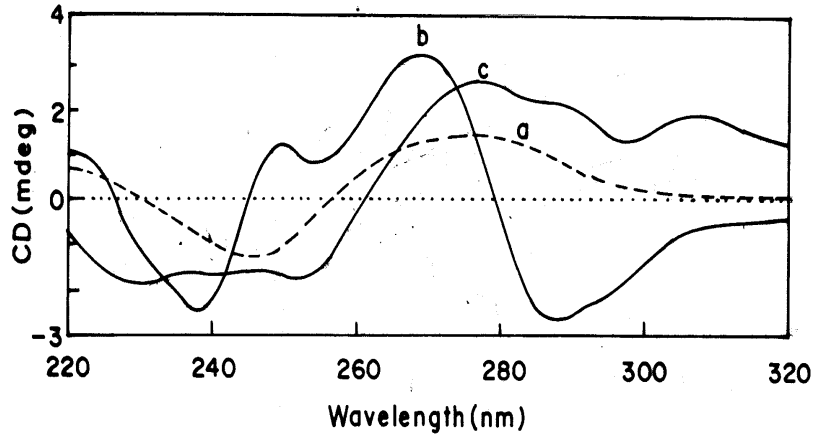

Figure S5B. Circular Dichroism spectra of CT DNA in the absence (a) and presence of *rac*-$[Zn(5,6\text{-dmp})_3]^{2+}$ at 1/R = 2 (b) and of CT DNA incubated with EthBr in the presence of *rac*-$[Zn(5,6\text{-dmp})_3]^{2+}$ at 1/R = 2 (c). Conc. of CT DNA = 2 x 10^{-5} mol.dm^3 .

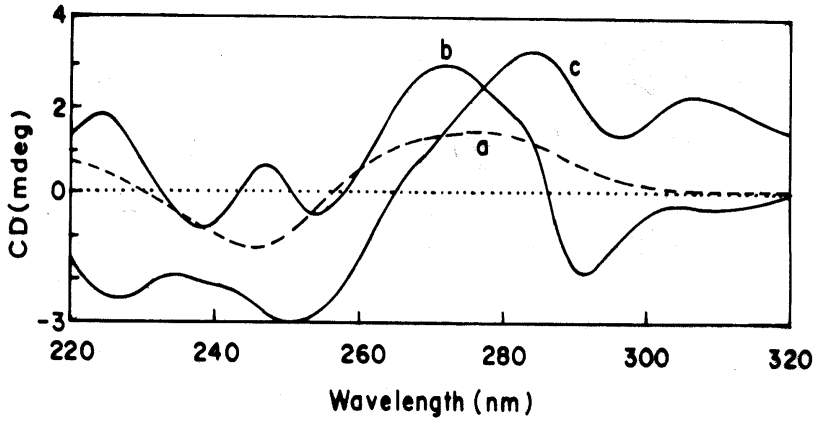

Figure S6A. Circular Dichroism spectra of CT DNA in the absence (a) and presence of *rac*-$[Cu(5,6\text{-dmp})_3]^{2+}$ at 1/R = 2 (b) and of CT DNA incubated with *rac*-$[Cu(phen)_3]^{2+}$ in the presence of *rac*-$[Cu(5,6\text{-dmp})_3]^{2+}$ at 1/R = 2 (c). Conc. of CT DNA = 2 x 10^{-5} mol.dm^3 .

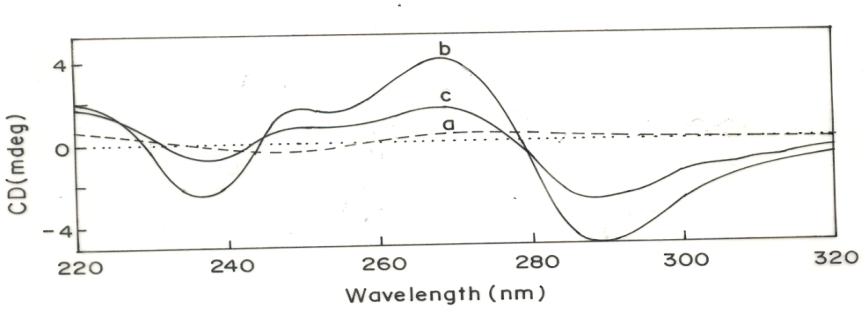

Figure S6B. Circular Dichroism spectra of CT DNA in the absence (a) and presence of *rac*-$[Cu(phen)_3]^{2+}$ at 1/R = 2 (b) and of CT DNA incubated with *rac*-$[Cu(5,6\text{-dmp})_3]^{2+}$ in the presence of *rac*-$[Cu(phen)_3]^{2+}$ at 1/R = 2 (c). Conc. of CT DNA = 2 x 10^{-5} mol.dm^3 .

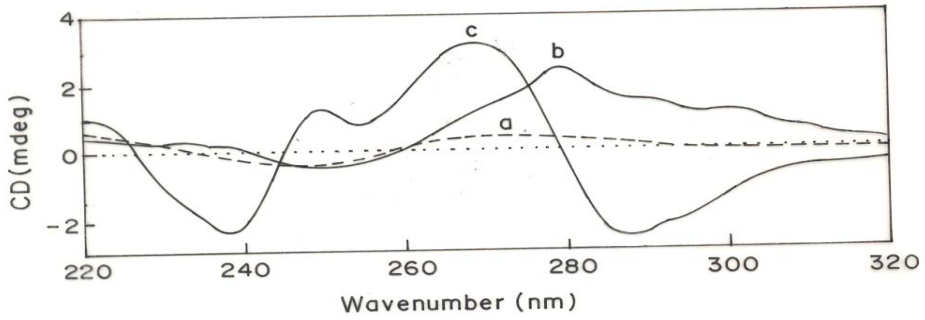

Figure S7A. Circular Dichroism spectra of CT DNA in the absence (a) and presence of *rac*-$[Zn(5,6\text{-dmp})_3]^{2+}$ at 1/R = 2 (b) and of CT DNA incubated with *rac*-$[Zn(phen)_3]^{2+}$ in the presence of *rac*-$[Zn(5,6\text{-dmp})_3]^{2+}$ at 1/R = 2 (c). Conc. of CT DNA = 2 x 10^{-5} mol.dm^3 .

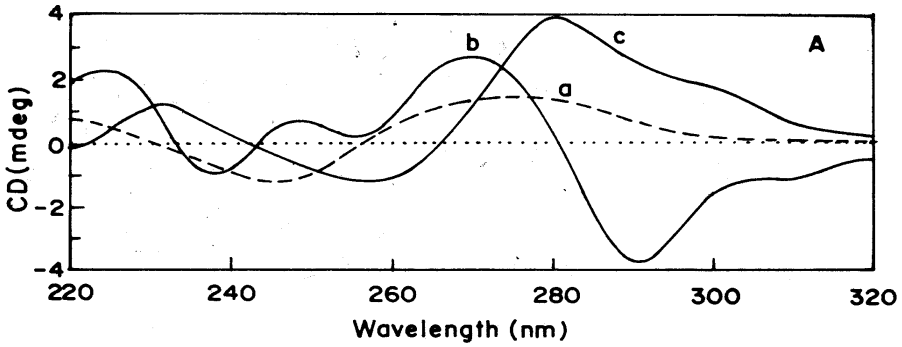

Figure S7B. Circular Dichroism spectra of CT DNA in the absence (a) and presence of *rac*-$[Zn(phen)_3]^{2+}$ at 1/R = 2 (b) and of CT DNA incubated with *rac*-$[Zn(5,6\text{-dmp})_3]^{2+}$ in the presence of *rac*-$[Zn(phen)_3]^{2+}$ at 1/R = 2 (c). Conc. of CT DNA = 2 x 10^{-5} mol.dm^3.

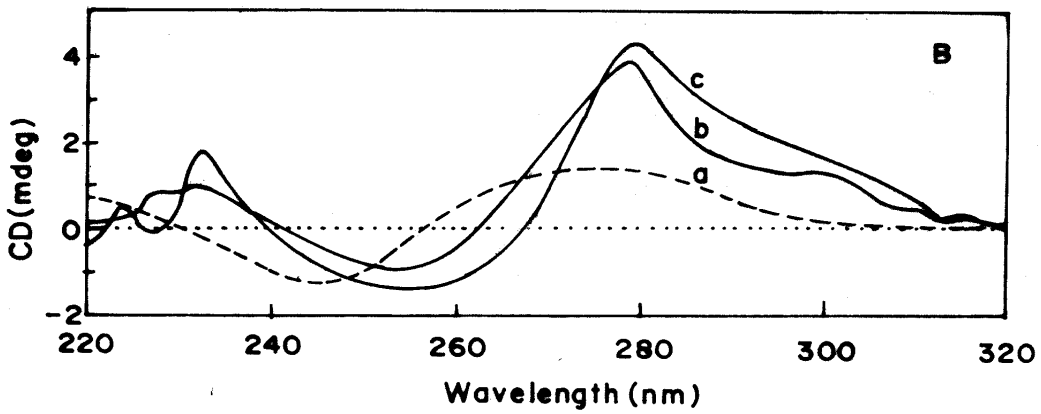

Figure S8A. Circular Dichroism spectra of CT DNA in the absence (a) and presence of *rac*-$[Cu(5,6\text{-dmp})_3]^{2+}$ at 1/R = 2 (b) and of CT DNA incubated with EDTA in the presence of *rac*-$[Cu(5,6\text{-dmp})_3]^{2+}$ at 1/R = 2 (c). Conc. of CT DNA = 2 x 10^{-5} mol.dm^3.

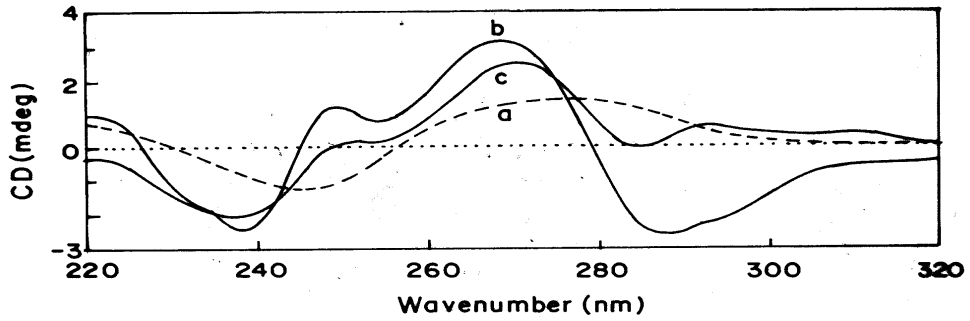

Figure S8B. Circular Dichroism spectra of CT DNA in the absence (a) and presence of *rac*-$[Zn(5,6\text{-dmp})_3]^{2+}$ at 1/R = 2 (b) and of CT DNA incubated with EDTA in the presence of *rac*-$[Zn(5,6\text{-dmp})_3]^{2+}$ at 1/R = 2 (c). Conc. of CT DNA = 2 x 10^{-5} mol.dm^3.

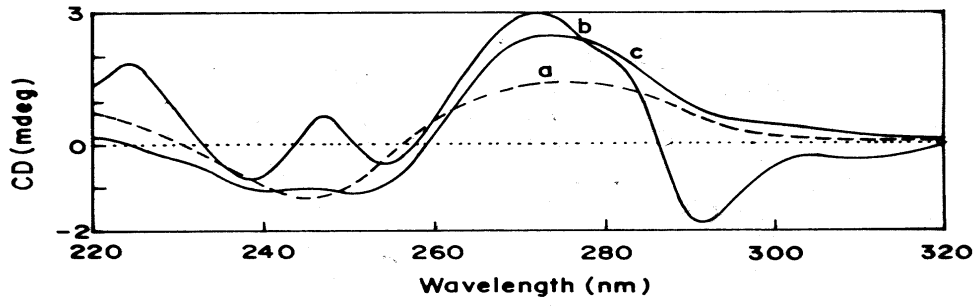

Figure S9. Cleavage of supercoiled pUC 19 DNA (40 μM) by the copper(II) complexes in 5% DMF : 5 mM Tris-HCl/50 mM NaCl at pH = 7.1 and 37 °C in the presence of ascorbic acid (H_2A, 10 μM) at 37 °C. Lane 1, DNA ; lane 2 + DNA + H_2A; lane 3, DNA + $[Cu(phen)_2Cl]Cl$ + H_2A; lane 4, DNA + **1** + H_2A; lane 5, DNA + $[Cu(5,6\text{-}dmp)_2Cl]Cl$ + H_2A; lane 6, DNA + **2** + H_2A; Complex concentration is 30 μM for lanes 2-7. Forms I and II are supercoiled and nicked circular forms of DNA respectively.

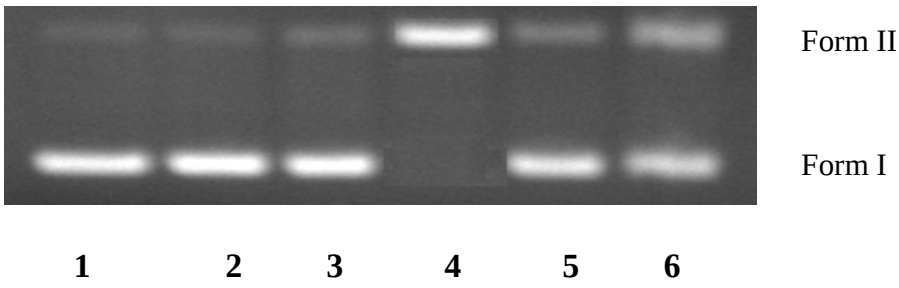

Figure S10A. Cleavage of supercoiled pUC19 DNA (40 μM) by complex **1** (10 – 30 μM) in 10% DMF / 5 mM Tris-HCl/50 mM NaCl at pH = 7.1 and 37 °C in the presence of ascorbic acid (H_2A, 10 μM) at 37 °C. Lane 1, + DNA + H_2A; lane 2, DNA + **1** (10 μM) + H_2A; lane 3, DNA + **1** (20 μM) + H_2A; lane 4, DNA + **1** (30 μM) + H_2A; lane 5, DNA + **1** (30 μM) + H_2A + 2 μL DMSO; Lane 6, DNA + **1** (30 μM) + H_2A + Distamycin. Forms I and II are supercoiled and nicked circular forms of DNA respectively.

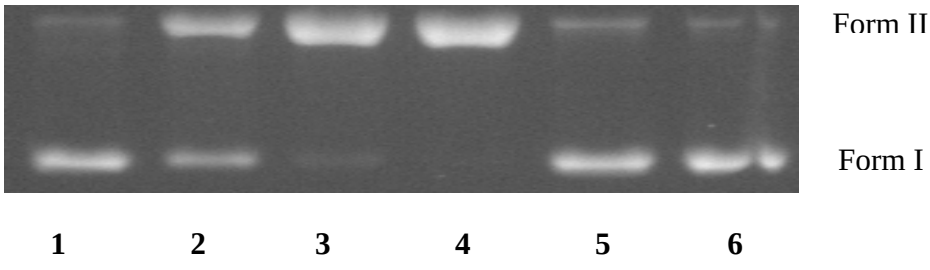

Figure S10B. Concentration dependent DNA (40 μM) cleavage by complex **1** (10 – 50 μM) in 10% DMF / 5 mM Tris-HCl/50 mM NaCl at pH = 7.1 and 37 °C in the presence of ascorbic acid (H_2A, 10 μM) at 37 °C. Lane 1, DNA ; lane 2, DNA + H_2A; lane 3, DNA + **1** (10 μM) + H_2A; lane 4, DNA + **1** (20 μM) + H_2A; lane 5, DNA + **1** (30 μM) + H_2A; lane 6, DNA + **1** (40 μM) + H_2A; lane 7, DNA + **1** (50 μM) + H_2A; Forms I and II are supercoiled and nicked circular forms of DNA respectively

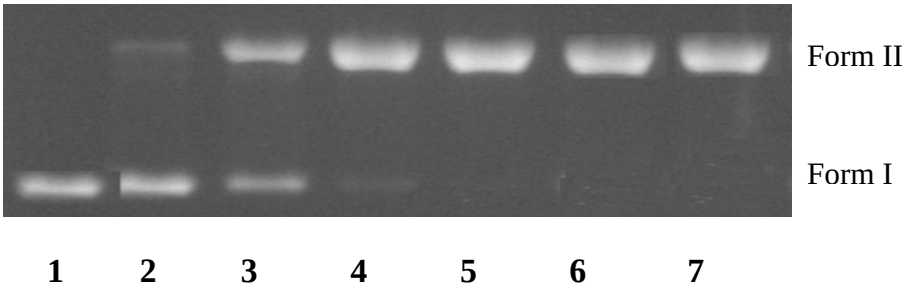

Figure S10C. Concentration dependent DNA (40 μM) cleavage by complex **1** (2 – 10 μM) in 10% DMF / 5 mM Tris-HCl/50 mM NaCl at pH = 7.1 and 37 °C in the presence of ascorbic acid (H_2A, 10 μM) at 37 °C. lane 1 + DNA + H_2A; lane 2, DNA + **1** (2 μM) + H_2A; lane3, DNA + **1** (4 μM) + H_2A; lane 4, DNA + **1** (6 μM) + H_2A; lane 5, DNA + **1** (10 μM) + H_2A; lane 7, DNA + **1** (8 μM) + H_2A; Forms I and II are supercoiled and nicked circular forms of DNA respectively

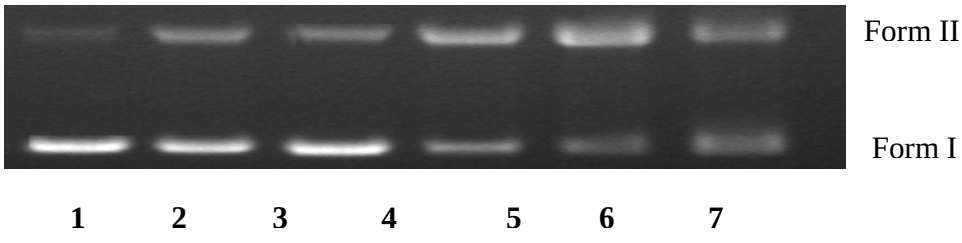

Figure S11. Concentration dependent DNA (40 μM) cleavage by the complex **2** (10 – 50 μM)in 5% DMF : 5 mM Tris-HCl/50 mM NaCl at pH = 7.1 and 37 °C in the presence of ascorbic acid (H_2A, 10 μM) at 37 °C. Lane 1, DNA ; lane 2, DNA + H_2A; lane 3, DNA + **2** (10 μM) + H_2A; lane 4, DNA + **2** (20 μM) + H_2A; lane 5, DNA + **2** (30 μM) + H_2A; lane 6, DNA + **2** (40 μM) + H_2A; lane 7, DNA + **2** (50 μM) + H_2A; ; lane 8, DNA + **2** (30 μM) + H_2A + 2 μL DMSO; Lane 9, DNA + **2** (30 μM) + H_2A + Distamycin. Forms I and II are supercoiled and nicked circular forms of DNA respectively.

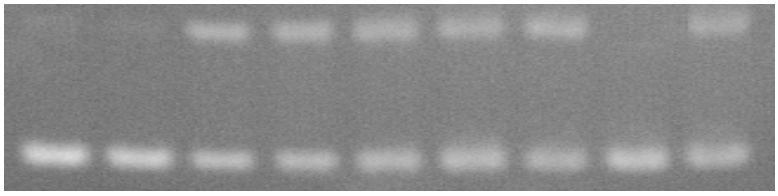

Figure S12. Concentration dependent DNA (40 μM) cleavage by the complex **3** (2 – 10 μM) in 10% DMF 5 mM Tris-HCl/50 mM NaCl at pH = 7.1 and 37 °C in the presence of ascorbic acid (H_2A, 10 μM) at 37 °C. Lane 1, DNA ; lane 2, DNA + H_2A; lane 3, DNA + **3** (2 μM) + H_2A; lane 4, DNA + **3** (4 μM) + H_2A; lane 5, DNA + **3** (6 μM) + H_2A; lane 6, DNA + **3** (8 μM) + H_2A; lane 7, DNA + **3** (10 μM) + H_2A; Forms I and II are supercoiled and nicked circular forms of DNA respectively

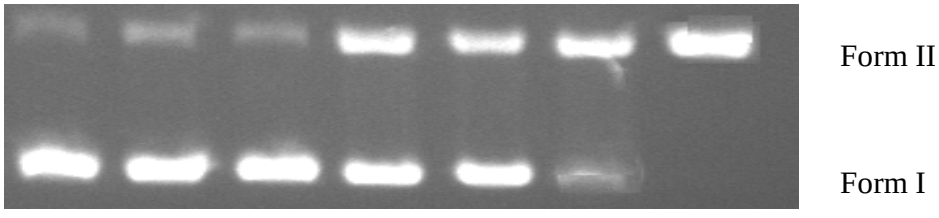

Figure S13. Concentration dependent DNA (40 μM) cleavage by the $[Cu(dpq)_2Cl]^{2+}$ complex (2 – 10 μM)in 5% DMF : 5 mM Tris-HCl/50 mM NaCl at pH = 7.1 and 37 °C in the presence of ascorbic acid (H_2A, 10 μM) at 37 °C. Lane 1, DNA ; lane 2 , DNA + H_2A; lane 3, DNA + $[Cu(dpq)_2Cl]^{2+}$ (2 μM) + H_2A; lane 4, DNA + $[Cu(dpq)_2Cl]^{2+}$ (4 μM) + H_2A; lane 5, DNA + $[Cu(dpq)_2Cl]^{2+}$ (6 μM) + H_2A; lane 6, DNA + $[Cu(dpq)_2Cl]^{2+}$ (8 μM) + H_2A; lane 7, DNA + $[Cu(dpq)_2Cl]^{2+}$ (10 μM) + H_2A.

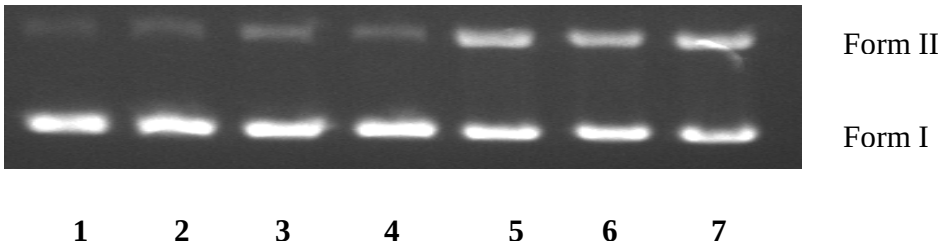

Figure S14. Cleavage of supercoiled pUC19 DNA (40 μM) by 10 μM complex (**1** – **3**) in 10% DMF / 5 mM Tris-HCl/50 mM NaCl at pH = 7.1 and 37 °C in the presence of H_2O_2 (200 μM) at 37 °C. Lane 1, DNA ; lane 2, DNA + H_2O_2 ; lane 3, DNA + H_2O_2 + **1**; lane 4, DNA + H_2O_2 + **3**; lane 5, DNA + H_2O_2 +**2**. Forms I and II are supercoiled and nicked circular forms of DNA respectively.

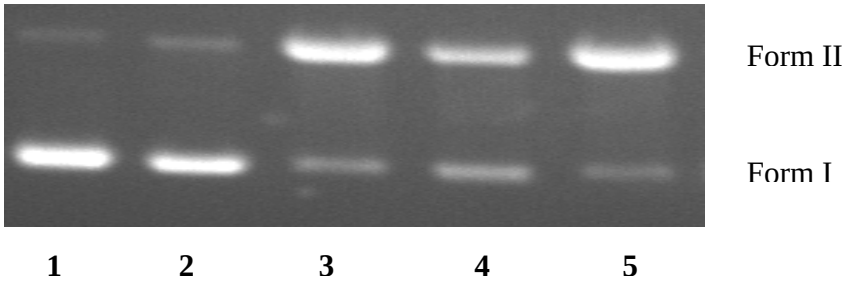

Figure S15. Cleavage of supercoiled pUC19 DNA (40 μM) by the copper(II) complexes in a 5 mM Tris-HCl/50 mM NaCl at pH = 7.1 and 37 °C in the presence of H_2O_2 (200 μM) at 37 °C. Lane 1, DNA + 2 μL DMSO; lane 2, DNA + H_2O_2 + 2 μL DMSO; lane 3, DNA + **1** + H_2O_2 + 2 μL DMSO; lane 4, DNA + **3** + H_2O_2 + 2 μL DMSO; lane 5, DNA + **2** + H_2O_2 + 2 μL DMSO; Complex concentration is 10 μM for lanes 3-5. Forms I, II and are supercoiled, nicked circular forms of DNA, respectively.

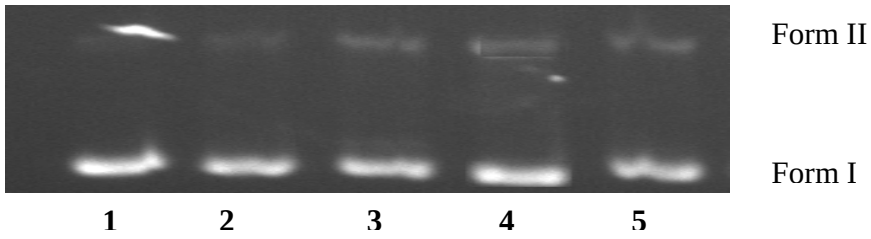

Figure S16. (A) Time dependent DNA (40 μM) cleavage by the complex **2** (10 – 60 min) in 10% DMF / 5 mM Tris-HCl/50 mM NaCl at pH = 7.1 and 37 °C in the presence of H_2O_2 (200 μM) at 37 °C. Lane 1, DNA + H_2O_2; lane 2, DNA + **2** (10 min) + H_2O_2 ; lane 3, DNA + **2** (20 min) + H_2O_2; lane 4, DNA + **2** (30 min) + H_2O_2; lane 5, DNA + **2** (40 min) + H_2O_2; lane 6, DNA + **4** (50 min) + H_2O_2; lane 7, DNA + **3** (60 min) + H_2O_2 ; Forms I and II are supercoiled and nicked circular forms of DNA respectively.